Am J Physiol Lung Cell Mol Physiol
280: L141–L151, 2001.

Surfactant protein A and lipid are internalized via the coated-pit pathway by type II pneumocytes

PAUL A. STEVENS,[1] HEIDE WISSEL,[1] STEFAN ZASTROW,[1]
DANIELA SIEGER,[1] AND KLAUS-PETER ZIMMER[2]
[1]*Clinic of Neonatology, University Children's Hospital Charité, Humboldt-Universität Berlin, 10098 Berlin; and* [2]*University Children's Hospital, Westfälische Wilhelms-Universität Münster, 48149 Münster, Germany*

Received 17 January 2000; accepted in final form 18 August 2000

Stevens, Paul A., Heide Wissel, Stefan Zastrow, Daniela Sieger, and Klaus-Peter Zimmer. Surfactant protein A and lipid are internalized via the coated-pit pathway by type II pneumocytes. *Am J Physiol Lung Cell Mol Physiol* 280: L141–L151, 2001.—Surfactant protein (SP) A and SP-A-mediated lipid uptake by isolated type II cells were investigated with biochemical and morphological methods. Inhibition of coated-pit function by potassium depletion severely reduced both SP-A and SP-A-mediated lipid internalization. Lipid uptake in the absence of SP-A was not affected. With confocal laser scanning microscopy and immunoelectron microscopy, SP-A and lipid predominantly (60%) colocalized in intracellular vesicles carrying early endosomal markers (EEA1) 5 min after endocytosis but were negative for the late endosomal or lysosomal marker LAMP-1. As estimated by subcellular fractionation, at this time point, 23% of the internalized SP-A and 45% of internalized lipid were localized within light (<0.38 M sucrose) fractions, which contain lamellar bodies and are positive for EEA1. The remaining label was predominantly found within EEA1-positive and plasma membrane-containing subfractions (≥1 M sucrose). We suggest that in isolated type II cells in vitro, SP-A and lipid are taken up together via the coated-pit pathway and that at early time points, both components reside in the same early endosomal compartment.

early endosome; lamellar body; coated vesicle

THE SURFACTANT-ASSOCIATED GLYCOPROTEIN surfactant protein (SP) A (molecular mass of 650 kDa under native conditions) plays an important role in the regulation of surfactant metabolism. Via an interaction with components of the type II cell membrane, it inhibits stimulated surfactant lipid secretion and stimulates surfactant lipid reuptake and recycling toward lamellar bodies, the secretory organelles of type II pneumocytes. Stevens et al. (22) and Wissel et al. (29) have recently described a SP-A-binding type II cell membrane protein (BP55), which is involved in surfactant lipid endocytosis. The precise mechanism by which the interaction of SP-A with its receptor stimulates lipid uptake, however, is not understood yet. Morphological studies (10–12, 19, 33) have demonstrated SP-A in association with coated pits and coated vesicles, suggesting receptor-mediated endocytosis of SP-A. Because of its high affinity for lipids and its liposome-aggregating properties, it seems conceivable that SP-A, on its internalization, could take lipids with it via the coated-pit internalization pathway.

To clarify these issues, we combined biochemical assays with confocal laser scanning microscopy (CLSM) and electron-microscopic techniques to study the internalization mechanisms and intracellular fate of the endocytosed components in freshly isolated type II cells. We found that inhibition of coated-pit formation by potassium depletion inhibited both SP-A and lipid internalization, suggesting that both surfactant components enter via the same mechanism involving clathrin-coated pits. As demonstrated by CLSM and immunoelectron microscopy and substantiated by subcellular fractionation experiments, at early time points after endocytosis, the protein and lipid colocalize in the same intracellular compartments, most likely early endosomes.

MATERIALS AND METHODS

Chemicals. Lipids, glutathione, fluorescein isothiocyanate (FITC), tetramethylrhodamine isothiocyanate-labeled *Maclura pomifera* lectin, FITC-labeled concanavalin A, and Lucifer yellow CH were obtained from Sigma (Deisenhofen, Germany). An early endosomal marker (EEA1) and cyanine-3-labeled anti-mouse IgG antibodies were obtained from Dianova (Hamburg, Germany). The mouse anti-clathrin heavy chain IgG antibody was obtained from Transduction Laboratories (Lexington, KY). The 2H5 anti-BP55 antibody was prepared as previously described (19). All radioactive isotopes as well as the BCS scintillation fluid were from Amersham (Braunschweig, Germany). Elastase and fatty acid-free bovine serum albumin fraction V were from Boehringer Mannheim (Mannheim, Germany). Cell culture media and supplements were from Life Technologies (Gaithersburg, MD). L-α-Phosphatidylethanolamine (PE)-*N*-(lissamine rhodamine B sulfonyl) (rhodamine-PE) was from Avanti Polar Lipids (Alabaster, AL). Biotin derivatives were from Pierce

Address for reprint requests and other correspondence: P. A. Stevens, Clinic of Neonatology, Univ. Children's Hospital, Charité-Campus Mitte, Humboldt-Univ. Berlin, Schumannstrasse 20-21, 10098 Berlin, Germany (E-mail: paul_a.stevens@charite.de).

The costs of publication of this article were defrayed in part by the payment of page charges. The article must therefore be hereby marked "*advertisement*" in accordance with 18 U.S.C. Section 1734 solely to indicate this fact.

(Rockford, IL). All other chemicals were of analytic grade from major suppliers.

Type II pneumocyte preparation. Type II cells were isolated from the lungs of adult male rats (body wt 120–140 g) according to Dobbs et al. (3). All in vitro experiments were done on freshly isolated cells in suspension.

Isolation of SP-A. SP-A was purified from lavages of fresh lamb lungs obtained from the local slaughterhouse as previously described (29). All samples used were tested for purity, contamination with immunoglobulins, lipid aggregation properties, and activity in surfactant secretion assays as previously described (29).

Labeling of SP-A. For biotinylation, SP-A was labeled with biotin derivatives (either NHS-LC-biotin or NHS-SS-biotin) at pH 6.3 as previously described (29).

SP-A was labeled with FITC as described by Benne et al. (1). The labeled SP-A was then divided into aliquots and frozen at −20°C.

Functional activity of all labeled SP-A batches was tested as described by Wissel et al. (30).

Liposome preparation. Small unilamellar liposomes containing 55% (by weight) dipalmitoylphosphatidylcholine (DPPC), 25% egg phosphatidylcholine, 10% dipalmitoylphosphatidylglycerol, and 10% cholesterol were made by sonication as previously described (29).

As a radioactive lipid marker, 1,2-dipalmitoyl-L-3-phosphatidyl-*N*-[*methyl*-^{3}H]choline, (1.46 nCi/μg lipid) was added. In some experiments, the liposomes were labeled with the fluorescent lipid rhodamine-PE added at 1%, and unlabeled PE was added at 1% in exchange for an equal amount of DPPC.

Potassium depletion. Potassium depletion of the cells was done according to Larkin et al. (16).

Disulfide-biotinylated SP-A internalization assay. Before the assay was started, the cell medium was changed once, the cells were cooled on ice, and then 3 μg/10^6 cells of SP-A labeled with NHS-SS-biotin (B-SS-SP-A) were incubated with the cells at 37°C for different periods of time as indicated in RESULTS, Figs. 1–5, and Tables 1 and 2. During the incubation period, the cells were continuously and gently shaken. Then, the medium was removed, and the cells were washed once with ice-cold PBS plus 10 mM EGTA (pH 7.4) for 5 min on ice. Subsequent removal of extracellular label was done by the glutathione-iodoacetamide method as described by Volz et al. (25). Equal amounts of total protein were subjected to SDS-PAGE under nonreducing conditions, blotted onto nitrocellulose, and visualized by enhanced chemiluminescence on film with avidin-peroxidase. The results were quantitated by scanning densitometry.

Liposome internalization assay. Liposome uptake assays were performed as described by Wissel et al. (29).

SP-A-binding assay. SP-A binding to type II cells was assayed at 3°C. In addition, calculation of the specific binding of SP-A under potassium-depleted and control conditions was performed by slope peeling (5) after incubation of the cells with labeled SP-A for 60 min at 37°C.

Lucifer yellow endocytosis. Potassium-depleted and control cells were incubated with 1 mg/ml of Lucifer yellow in control or potassium-depleted buffer for 0, 5, or 15 min at 37°C. The cells were washed twice in PBS-1% BSA and twice in PBS at 4°C and then lysed in PBS-0.3% Triton X-100. Intracellular Lucifer yellow concentration was determined by fluorescence spectrometry (excitation at 430 nm and emission at 540 nm).

CLSM. At each time point, 5×10^6 type II cells suspended in 1 ml of DMEM-0.1% BSA were incubated with 100 μg of liposomal phospholipid containing rhodamine-PE and 5 μg of FITC-SP-A. Further procedures for CLSM are described in Fig. 3. The cells were examined with an epifluorescence microscope interfaced with a CLSM (Leica CLSM, Leica Lasertechnic, Heidelberg, Germany) equipped with an argon-krypton laser. Images of the cells were created with standard objectives and photomultiplier tubes dedicated to fluorescent excitation and emission spectra for rhodamine (excitation 541 nm and emission 572 nm) and FITC (excitation 490 nm and emission 520 nm). With the dual-channel system of the confocal microscope, dual-emission (535/590 nm) images were recorded simultaneously with a scanning speed of 16 s/frame (512 lines). Serial sectioning of cells at a depth of 0.5 μm was performed to distinguish material adhering to the cell membrane from internalized material and to assess intracellular colocalization of SP-A and lipid.

All experiments were repeated five times; for each experiment, at least 10 cells were evaluated.

Electron microscopy. Detection of coated pits and coated vesicles of isolated type II pneumocytes was performed on Epon sections processed by standard techniques. Potassium-containing and -depleted cells were treated with 1 μg/ml of SP-A for 10, 20, and 30 min. The number of coated pits and coated vesicles per 40-nm section of the cell was determined by an investigator blinded to the treatment group.

For intracellular localization experiments, type II cells were incubated with 4 μg FITC-labeled SP-A/10^6 cells at 37°C under either potassium-containing or -depleted conditions for 5 or 10 min. Localization of FITC-labeled SP-A on thin frozen sections of type II cells was done with the technique of Tokuyasu as previously described (35). The cells were cooled down to 3°C, washed, and fixed in 5% paraformaldehyde-250 mM HEPES, pH 7.4. The frozen sections were labeled with a polyclonal rabbit (1:150 dilution; Molecular Probes Europe, Leiden, The Netherlands) and a monoclonal mouse (1:30 dilution) antibody against FITC. A monoclonal mouse antibody against rat LAMP-1 (GM10) was taken to identify late endosomes and lysosomes. The binding sites of the antibodies were indicated by goat anti-rabbit or anti-mouse serum conjugated with 6- or 12-nm large gold particles (1:10 dilution) in a Philips 301 electron microscope.

For in situ localization, 80 μg of FITC-labeled SP-A in 1 ml of PBS were instilled intratracheally in vivo into the lungs of a deeply anesthetized rat 5 min before death. The lungs were perfused first with an ice-cold solution containing 140 mM NaCl, 5 mM KCl, 2 mM $CaCl_2$, 1.3 mM $MgSO_4$, 2.5 mM sodium phosphate, 10 mM HEPES, and 6 mM glucose, pH 7.4, until they were blood free and subsequently with ice-cold 5% paraformaldehyde fixating solution. After removal from the thorax, the lungs were then lavaged twice with the fixating solution and put into a 15-ml test tube filled with paraformaldehyde solution. They were then cut and prepared for Epon and thin frozen sections as described above.

Distribution of endocytosed lipid in subcellular fractions. After uptake of labeled liposomes in the presence and absence of B-SS-SP-A, the cells were washed, and the subcellular fractions were separated by sucrose gradient centrifugation with the procedure described by Duck-Chong (4). For this, the lysate in 1 M sucrose was overlaid with 1-ml fractions of sucrose solutions of decreasing molarity (from bottom to top 0.8–0.2 M). The gradient was then centrifuged at 60,000 *g* for 2 h in a Beckman ultracentrifuge (SW 41 rotor). After completion, the sucrose fractions were taken off in 1-ml fractions. The refraction index of each fraction was determined, and the corresponding molarity was calculated. In each fraction, radioactivity and protein content were measured as described in *Liposome internalization assay*. SP-A was visualized on blots as described in *Disulfide-biotinylated SP-A internalization assay*.

Data analysis. All results are means ± SE. Statistical analysis was done with paired and unpaired *t*-tests. For multiple comparisons, analysis of variance with subsequent Fisher's protected least significant difference test was used. The level of significance was set at $P < 0.05$.

RESULTS

Potassium depletion. As determined by atom emission spectrometry, control cells contained 0.056 mmol/l of potassium. Depletion led to an eightfold decrease in intracellular potassium content after 60 min (0.0064 mmol/l).

As determined by trypan blue exclusion and lactate dehydrogenase release, this procedure did not damage the cells to a significant extent. Dye was excluded in 97.3 ± 0.5% of the untreated cells, 93 ± 1% of the control cells, and 91 ± 1% of the potassium-depleted cells. Vitality after 20 min of incubation with lipids and SP-A was 91 ± 1% in the control group and 89 ± 1% in the potassium-depleted group. Less than 2% of the total cellular lactate dehydrogenase content was released during the course of the experiment in either group ($n = 3$ experiments with duplicate measurements).

The protein content of the cells was not altered by the procedure (control cells, 141 ± 0.9 μg/2.5 million cells vs. potassium-depleted cells, 145 ± 2.2 μg/2.5 million cells).

Effect of potassium depletion on protein synthesis and intracellular energy stores. After hypotonic shock and incubation in potassium-free or potassium-containing medium for 20 min, the cells were incubated with 10 μCi of [^{3}H]leucine added to the medium for 4 h. After precipitation with trichloroacetic acid, the amount of total cellular protein was measured, and incorporation of label in the protein pellet was measured by liquid scintillation counting as described in MATERIALS AND METHODS. Incorporation of labeled leucine into potassium-depleted cells was 8–10 times lower than in potassium-containing cells ($n = 3$ experiments). These values are in accordance with the literature (17).

To test whether protein synthesis was needed for lipid endocytosis at short time points, lipid uptake by type II cells with time was measured in the presence of 100 mM cycloheximide, a protein synthesis inhibitor. For periods of up to 2 h, lipid uptake by type II cells as assessed by incorporation of [^{3}H]DPPC or [^{14}C]cholesterol ester in either the presence or absence of SP-A was not affected by inhibition of de novo protein synthesis ($n = 6$ experiments; results not shown).

As an additional control, ATP content was determined in control and potassium-depleted cells according to Jaworek et al. (9). Potassium depletion slightly reduced the ATP content of type II cells from 20.92 ± 2.6 to 18.37 ± 0.73 nmol/mg protein ($n = 3$ experiments; results not significant).

Effect of potassium depletion on coated-pit formation. Freshly isolated type II cells were incubated in the presence of SP-A (4 μg/10^{6}cells) under either control or potassium-depleted conditions at 37°C for various periods of time. Thereafter, the cells were then prepared for electron microscopy (see MATERIALS AND METHODS). At each time point, 20 cells were used for counting by an investigator blinded to the treatment. As shown in Table 1, potassium depletion led to a severe reduction of the number of coated pits and especially of coated vesicles per 40-nm section.

Effect of inhibition of coated-pit formation on SP-A uptake. In preliminary experiments, we had found that adding a 100-fold excess of unlabeled SP-A together with the biotin-labeled SP-A to the cells completely inhibited the binding of labeled SP-A to the cells. Also, incubating the cells with SP-A in the presence of 10 mM EDTA resulted in a 95% decrease in binding of SP-A to the cells. This result is in accordance with those of other authors (14, 31). Washing the cells with 10 mM EDTA after preincubation of the cells with SP-A for 30–60 min only removed 55–60% of the label. Because this amount of label adhering nonspecifically to the cells would have impaired our efforts to investigate intracellular trafficking of endocytosed labeled SP-A, we adapted an assay using a disulfide-linked biotin label previously characterized in other cell systems (2, 25) for use in our system. Inclusion of EGTA washes in-between proved necessary to remove all of the labeled SP-A, probably because in our setup, large aggregates of SP-A, which cannot be completely penetrated by glutathione, were formed at the cell membrane with time.

Figure 1 shows the time course of SP-A uptake under normal (potassium-containing) conditions with the B-SS-SP-A assay (3 μg SP-A/1 × 10^6 cells; $n = 5$ experiments). Within minutes, intracellular B-SS-SP-A levels rose sharply and had not yet reached a maximum at 20 min. Potassium depletion, in contrast, led to a severe reduction in SP-A internalization. B-SS-SP-A levels in potassium-depleted cells were 17.6% of the normal value at 10 min ($P < 0.0001$) and 20% at 20 min ($P < 0.0001$). This was confirmed by CLSM with FITC-labeled SP-A. By immunoelectron microscopy, as shown in Fig. 2, at these early time points, SP-A was found in coated pits (Fig. 2*A*) and coated vesicles (Fig. 2*B*). Very little label was detected within the cells after potassium depletion (see Fig. 3*F*). Potassium depletion did not influence internalization of the fluid-phase

Table 1. *No. of coated pits and vesicles in potassium-depleted and control cells*

	0 Minute	10 Minutes	20 Minutes	30 Minutes
Control				
Coated pit	0.85 ± 0.21	1.3 ± 0.21	1.10 ± 0.27	1.97 ± 0.26
Coated vesicle	0	0.1	0.13	0.13
Potassium depleted				
Coated pit	0.75 ± 0.16	ND	0.45 ± 0.25	0.55 ± 0.25*
Coated vesicle	0	ND	0	0

Values are means ± SE of occurrences/40-nm section; $n = 20$ cells/time point. Experiments were done in the presence of 1 μg/ml of surfactant protein A (SP-A). ND, not detected. *$P < 0.05$ vs. potassium depleted.

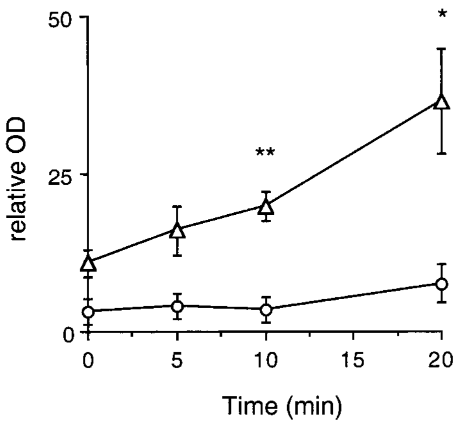

Fig. 1. Uptake of biotinylated surfactant protein (SP)-A in type II cells under potassium-depleted (○) and control (△) conditions as described in MATERIALS AND METHODS. Disulfide-biotinylated SP-A (3 μg/10^6 cells) was added at 37°C for indicated times. Cells were then washed as described in MATERIALS AND METHODS. SP-A was identified in Western blots by neutravidin-peroxidase and enhanced chemiluminescence. Results were quantitated by densitometry and are means ± SE expressed as relative optical density (OD); $n = 5$ experiments. *$P < 0.0001$ vs. potassium-depleted cells. **$P = 0.0105$ vs. potassium-depleted cells.

marker Lucifer yellow (Fig. 3*G*). As confirmed by fluorescence spectrometry, under control conditions after 15 min at 37°C, 10.7 ng Lucifer yellow/10^6 cells were internalized compared with 12.0 ng/10^6 cells under potassium-depleted conditions (not significant).

Although at 0 min, there was very little SP-A associated with the cells under potassium-depleted conditions [relative optical density (OD) 3.9 ± 1.9], under control conditions, more label remained associated with the cell membrane (relative OD 10.8 ± 2.2). SP-A-binding assays done at 3°C showed no significant difference between potassium-containing and -depleted cells (relative OD 57 ± 5.3 and 40 ± 3.6, respectively; $n = 4$ experiments). We also calculated specific high-affinity binding by slope peeling under potassium-depleted and control conditions at 37°C for 60 min. Again, no significant differences could be found between binding affinities for both conditions (concentrations causing half-maximal binding: control condition, 1.45 μg/ml; potassium-depleted condition, 1.35 μg/ml; $n = 4$ experiments). Total binding was slightly but not significantly lower in potassium-depleted cells versus control cells. Decreased binding of SP-A, therefore, cannot explain the inhibition of internalization seen in potassium-depleted cells.

Up to 120 min after the start of the uptake period, degradation products of biotinylated SP-A could not be demonstrated on SDS-PAGE and Western blots against streptavidin-peroxidase with the enhanced chemiluminescence system.

Effect of inhibition of coated-pit formation on lipid uptake. As shown in Fig. 4, SP-A-mediated lipid uptake (DPPC-labeled liposomes; $n = 9$ experiments) was severely reduced under potassium-depleted conditions compared with control conditions. Under control conditions, the amount of cell-associated DPPC that could not be removed from the cells increased from 153 ± 18.0 pmol/10^6 cells at 0 min to 576.8 ± 33.8 pmol/10^6 cells at 10 min ($P < 0.0001$ vs. 0 min) to 806.0 ± 6.8 pmol/10^6 cells after 20 min ($P < 0.0001$ vs. 0 min). Under potassium-depleted conditions at 0 min, 126.2 ± 18 pmol DPPC/10^6 cells were associated with the cells vs. 252.4 ± 15.8 pmol/10^6 cells at 10 min and 297.4 ± 27 pmol/10^6 cells at 20 min.

Expressed as the fraction of uptake under control conditions, the uptake under potassium-depleted conditions was ≈83% of that under control conditions at 0 min. This fraction decreases to 44% at 10 min and 37% at 20 min.

In the absence of SP-A, on the other hand, time-dependent association of labeled liposomes with type II cells was not different between both conditions. Although under normal control conditions, DPPC uptake increased from 3.8 ± 0.3 dpm/μg protein (85 ± 7 pmol/10^6 cells) at 0 min to 13.1 ± 1.5 dpm/μg protein (295.9 ± 3 pmol/10^6 cells) at 20 min, DPPC uptake under potassium-depleted conditions was only slightly lower (3 ± 0.2 dpm/μg protein at 0 min vs. 10.8 ± 1

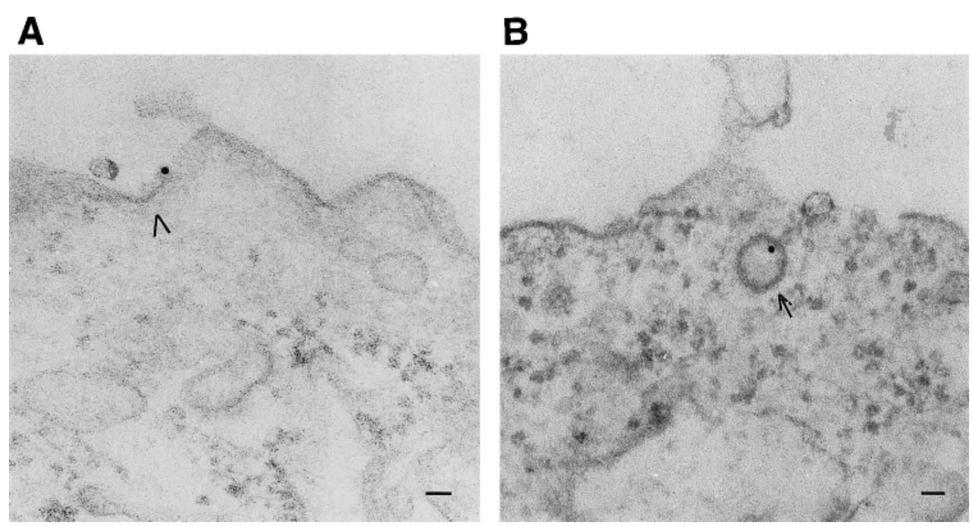

Fig. 2. Electron micrograph closeup of SP-A-containing coated pits and coated vesicles in isolated type II pneumocytes. After incubation with FITC-labeled SP-A (in the presence of lipids), Epon sections of isolated type II cells were incubated with a mouse anti-FITC antibody and goat anti-mouse antiserum conjugated with 12-nm large gold particles. *A*: closeup of clathrin-coated pit containing immunogold particle, indicating labeled SP-A (arrowhead). *B*: closeup of intracellular clathrin-coated vesicle containing immunogold particle, indicating endocytosed SP-A (arrow). Bars, 0.1 μm.

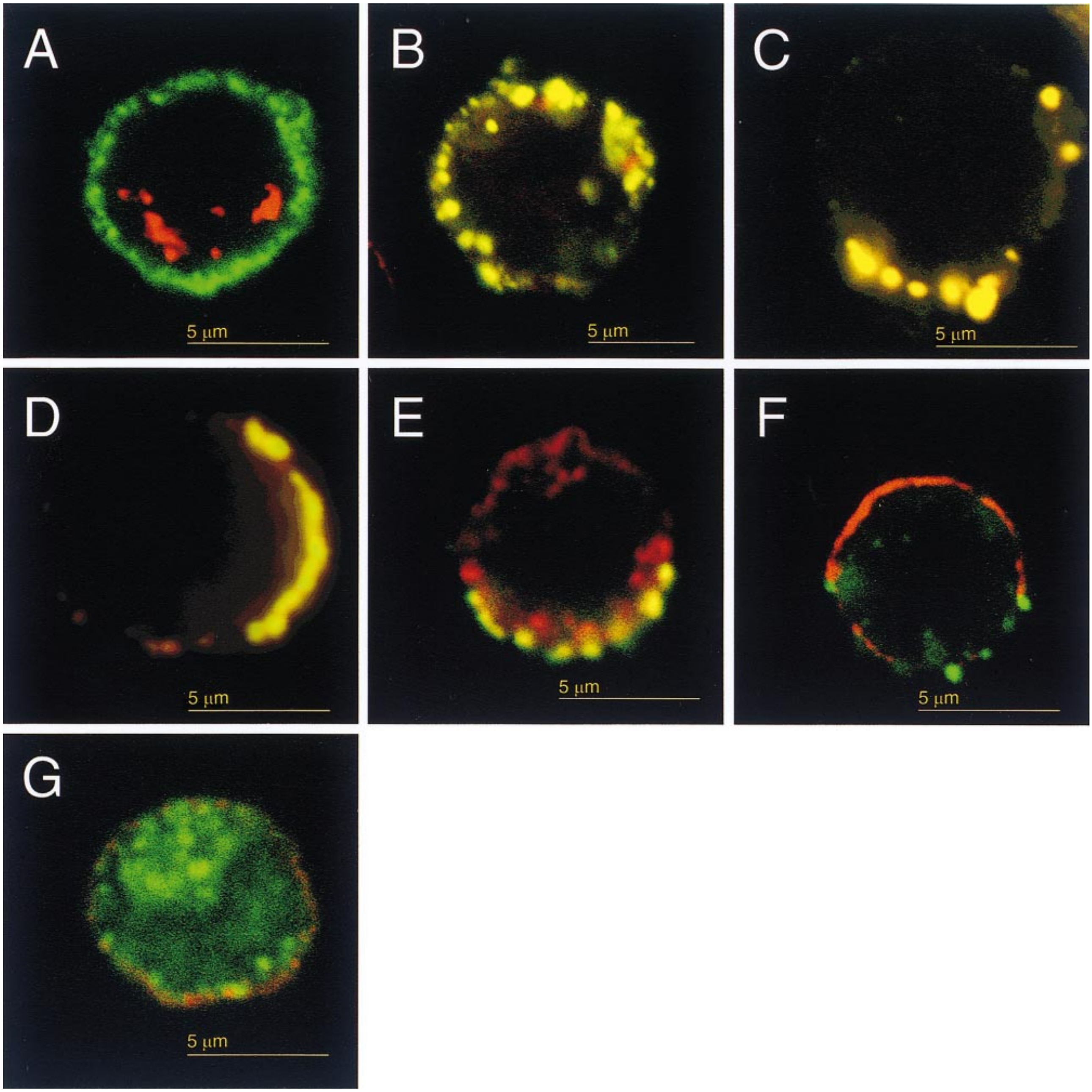

Fig. 3. Colocalization of endocytosed SP-A and lipids and of endocytosed SP-A and early endosomal markers in type II cells by confocal laser scanning microscopy. To demonstrate true intracellular localization of the internalized lipid components, freshly isolated type II cells were incubated with unlabeled SP-A and rhodamine-phosphatidylethanolamine (PE)-labeled liposomes for 3 min at 37°C and then incubated at 3°C for 30 min with FITC-labeled concanavalin A to visualize the cell boundaries (*A*). Cells were incubated with rhodamine-PE-labeled liposomes and FITC-labeled SP-A for 5 min at 37°C (*B*). To demonstrate colocalization of SP-A with clathrin, type II cells were incubated with FITC-labeled SP-A for 3 min at 37°C and subsequently with anti-clathrin antibody and cyanine-3 (Cy3)-labeled anti-mouse IgG antibody (*C*). Incubation of type II cells with SP-A for 5 min at 37°C and subsequently with the anti-BP55 antibody 2H5 and Cy3-labeled anti-mouse IgG showed colocalization of SP-A and its receptor BP55 at early time points (*D*). Freshly isolated type II cells (5×10^6) were incubated with 5 μg of FITC-labeled SP-A for 5 min at 37°C and subsequently with the antibody to the early endosomal marker EEA1 and Cy3-labeled anti-mouse IgG antibody (*E*). FITC-labeled SP-A was incubated with potassium-depleted type II cells for 15 min at 37°C and then incubated for 30 min at 3°C with tetramethylrhodamine isothiocyanate-labeled *Maclura pomifera* antigen to demonstrate internalization of SP-A within the cell boundaries (*F*). Potassium-depleted type II cells were incubated with 1 mg/ml of Lucifer yellow for 15 min at 37°C and then with *Maclura pomifera* as described above (*G*). Sections were made through the center of the cells.

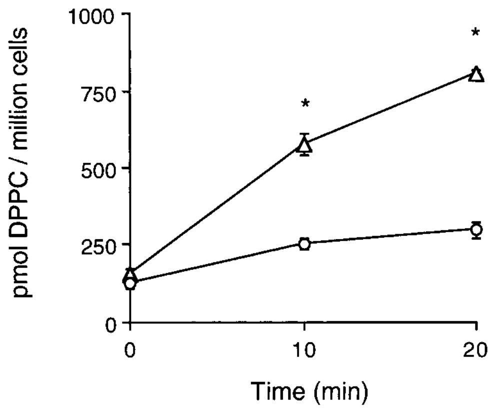

Fig. 4. Uptake of [^{3}H]dipalmitoylphosphatidylcholine (DPPC)-labeled lipids in the presence of SP-A in type II cells under potassium-depleted (○) and control (△) conditions. Type II cells were incubated with labeled liposomes and 2 μg SP-A/10^6 type II cells for different periods of time as described in MATERIALS AND METHODS. Lipid uptake assay was performed as described in MATERIALS AND METHODS. Values are means ± SE; $n = 9$ experiments. *$P < 0.0001$ vs. potassium-depleted cells.

dpm/μg protein at 20 min; 68 ± 5 pmol/10^6 cells at 0 min vs. 244 ± 2 pmol/cells at 20 min; not significant). Expressed as a fraction of uptake under potassium-containing conditions, uptake under potassium-depleted conditions remained ~80% at all time points.

By subtracting this latter value from the uptake values attained in the presence of SP-A, it became obvious that potassium depletion inhibited the SP-A-mediated lipid uptake completely (e.g., uptake after 20 min in the presence of potassium and SP-A, 806 pmol/10^6 cells; in the presence of potassium without SP-A, 295 pmol/10^6 cells; in the absence of potassium with SP-A, 297 pmol/10^6 cells).

Subcellular distribution of endocytosed surfactant components. Subcellular distribution of the SP-A and lipids endocytosed after different periods of internalization was investigated by subcellular fractionation with sucrose gradients. Total uptake of both labels in the continuous presence of extracellular label increased significantly with time, and a significant shift in the distribution of the internalized labels could be observed (Table 2). At 0 min, incubations were done at 3°C. Only fractions ≥ 1 M contained substantial amounts of SP-A and lipid at this time point.

As a control for unspecific cosedimentation, either liposomes or liposomes plus SP-A were added to the homogenized cells, and distribution of the lipid label in the different fractions was determined after centrifugation. If liposomes alone were added, most of the label (~84%) was found in the heavy (>0.76 M) fractions. Less than 1% of the label was found in the 0.22–0.32 M fraction and ~5% was found in the 0.33–0.48, 0.49–0.58, and 0.59–0.75 M fractions. The results for liposomes plus SP-A were similar to those with liposomes alone and substantially different from those obtained after 5 min of internalization. After 5 min of internalization, lipid and SP-A were found almost exclusively in the 0.2–0.48 and 0.76–1 M fractions, which were positive for the early endosomal marker EEA1. Strikingly, the lightest fraction (0.2–0.32 M) had the steepest increase in lipid label incorporation, suggesting that this fraction (and the 0.33–0.48 M fraction) was preferentially labeled at this early time point. Taken together, these results suggest that at least a substantial fraction of the early endosomes are contained within the 0.22–0.48 M fractions.

The results further suggest that the SP-A and lipid labels behaved differently on internalization. After 5 min at 37°C, 10.4% of the SP-A label was found in the lightest fraction (0.2–0.32 M); 12.5% of the SP-A label was found in the 0.33–0.48 M fraction, corresponding to lamellar bodies; 8.4% of the SP-A label was found in the 0.49–0.58 M fraction; and 37% of the SP-A label was found in the 0.76–1 M fraction. In contrast, after 5 min of internalization at 37°C, 18.1% of the lipid label was found in the light 0.2–0.32 M fraction, 27% in the 0.33–0.48 M lamellar body fraction, and 9.2% in the 0.49–0.58 M fraction. In the combined 0.76–1 M fraction, 25% of the total cell-associated label was found. It therefore seems that after 5 min of internalization, the lighter fractions are relatively enriched in lipid versus SP-A.

Colocalization of SP-A and lipid. We and others (10) have observed that in internalization experiments, a

Table 2. *Localization of SP-A and lipids in type II cell subcellular fractions*

Fraction	EEA1 Labeling	0 Minutes		5 Minutes		Increase vs. 0 Minute
		SP-A	Lipid	SP-A	Lipid	
0.2–0.32 M	9.5		1.5 ± 1.7	10.4 ± 2.6	18.1 ± 3.6	200×
0.33–0.48 M	4.4		2.6 ± 1.7	12.5 ± 1.3	27 ± 2.8	114×
0.49–0.58 M	0.08		2.2 ± 1.6	8.4 ± 1.2	9.2 ± 1.3	100×
0.59–0.75 M	0.07		2.4 ± 1.8	7.3 ± 1.6	8.7 ± 0.6	79×
0.76–0.99 M	4.2		1.7 ± 1.0	7.3 ± 1.7	5.5 ± 1.5	74×
1 M	35.4	10.8 ± 0.9	15 ± 10	29.3 ± 3.0	19.8 ± 1.7	28×
Pellet	46.4	89.2 ± 0.9	65 ± 15	24.8 ± 2.9	11.6 ± 3.9	0.54×

Values are means ± SE in percent of total; $n = 4$ independent experiments/time point. Type II cells (80×10^6) were incubated with 3 μg disulfide-biotinylated surfactant protein A (SP-A)/10^6 cells labeled in the presence of radioactively labeled liposomes for indicated times, and subcellular fractions were prepared. Gradient fractions were labeled with antibody against the early endosomal marker EEA1 as determined by Western blotting. Percentages of total internalized SP-A and lipid were determined as described in MATERIALS AND METHODS. For the increase vs. 0 min, the specific activity of the lipid in a fraction at 5 min was divided by the specific activity in that fraction at 0 min. Total amount of lipid label incorporated in the whole homogenate at 5 min was ~11 times that incorporated at 0 min.

fraction of the isolated type II cells do not contain endocytosed surfactant components. Using fluorescence microscopy, we found that ~73.3 ± 3% of the isolated type II cells had internalized SP-A as shown by the presence of the intracellular FITC label and that ~85% of the cells had internalized lipid, leaving ≈15% of the cells without any label (n = 17 experiments).

The cells in all our samples showed very little, if any, SP-A or lipid label adhering to the cell membrane, confirming the effectivity of our washing procedure to remove membrane-adhering material.

As shown by CLSM, after 3–5 min, substantial amounts of SP-A and lipid had been internalized and could be seen intracellularly in small vesicular structures near the periphery of the cells. Also, most of the vesicles (60%) contained both markers, therefore suggesting colocalization of SP-A and lipid at early time points (Fig. 3, *A* and *B*). Combining FITC-labeled SP-A and a monoclonal antibody against the early endosomal marker EEA1, we demonstrated that in isolated type II cells 5 min after the start of incubation, intracellular FITC-SP-A colocalized with EEA1, i.e., in early endosomes. (Fig. 3*E*). Also, at these early time points, the SP-A receptor BP55 (Fig. 3*D*) and clathrin (Fig. 3*C*) colocalized with SP-A and lipid. The colocalization of SP-A with clathrin-coated pits and vesicles was further demonstrated by electron microscopy (Fig. 2). These data therefore strongly suggest that at early time points after internalization, lipid and SP-A colocalize in intracellular vesicles along the clathrin-coated pit-early endosome pathway.

To further investigate the internalized components, immunoelectron microscopy was used on Epon sections as well as on cryosections of isolated type II cells. The ultrastructure of type II cells was well preserved on Epon sections as well as on cryosections.

Epon sections of type II cells incubated with FITC-labeled SP-A for 5 min showed a significant number of gold particles within most of the lamellar bodies (Fig. 5*A*). Also, in frozen sections in these experiments, strong labeling was found within large vacuoles filled with densely packed vesicles of intermediate size close to the cell surface of alveolar type II cells (Fig. 5*B*). They did not resemble multivesicular bodies, which are characterized by internal vesicles of smaller size containing a dense network of membranes that were not arranged in parallel orientation, as in the case in Epon sections of lamellar bodies, but were included in densely packed vesicles. Due to the high lipid content of the lamellar bodies, the stacked membranes of these organelles were only exceptionally visible in the cryosections as shown by others (22). Because SP-A was mainly localized within the large vacuoles containing many vesicles of intermediate size in thin frozen sections and within lamellar bodies in Epon sections, we tentatively conclude that the large vacuoles with the vesicles of intermediate size corresponded to lamellar bodies of cryosections. Simultaneous labeling of FITC-labeled SP-A and LAMP-1 with immunogold preparations from different species and gold particles did not show any colocalization within these organelles at these early time points.

As pointed out by Young et al. (33), the results from in vitro studies have to be interpreted with caution and compared with the in vivo situation. To confirm that the endocytic pathways and the organelles involved in our in vitro system were similar to the in vivo situation, we therefore performed an in vivo instillation study into intact lung. Significant qualitative differences between both systems were not detected. As expected, the alveolar lumen contained significant label. The same intracellular labeling pattern was found in the in situ lung as in the in vitro cell system. SP-A did not label any cell organelles other than the ones described in our in vitro system. Also, as in the in vitro system, in the in vivo lung, no colocalization of FITC-labeled SP-A and LAMP-1 could be found at early time points (~5 min after internalization).

DISCUSSION

SP-A stimulates lipid uptake by type II cells in vitro by a complex mechanism that is not well understood (24, 29). SP-A binds to high-affinity binding sites (receptors) at the type II pneumocyte cell membrane (15, 32) and has been demonstrated in association with coated pits and coated vesicles, suggesting receptor-mediated endocytosis via the coated-pit pathway (19).

SP-A does bind to lipids and in the presence of calcium causes aggregation of liposomes (6). A model of SP-A-mediated lipid uptake could therefore be constructed in which SP-A first binds to lipids and aggregates liposomes in the extracellular space. On its internalization via the coated-pit pathway, SP-A would then take these associated lipids with it.

We chose to test this model with a variety of complementary techniques. In a first approach, uptake via coated pits was disturbed by potassium depletion of the cells.

As described for other cell types (16, 17), potassium depletion of type II cells leads to a severe reduction in coated pits and especially in coated vesicles (Table 1). The influence of potassium depletion on coated-pit formation is only partially understood, involving abnormal clathrin polymerization into nonfunctional microcages (16). The procedure is reversible: on restoring the normal extracellular potassium content, the intracellular potassium concentration will restore itself, with a concomitant regain of functions affected by depletion (see RESULTS).

Our results demonstrate that in potassium-depleted type II cells, SP-A internalization is drastically reduced (Fig. 1), confirming what morphological work from other groups had suggested (10–12, 19, 33). Interestingly, coated-pit depletion also led to inhibition of SP-A-mediated lipid uptake, even though SP-A was present in the extracellular space and could still bind to its receptor. This argues against SP-A simply bringing lipids in close proximity to the cell membrane as the explanation for the enhanced lipid uptake in the presence of SP-A as suggested by Horowitz and col-

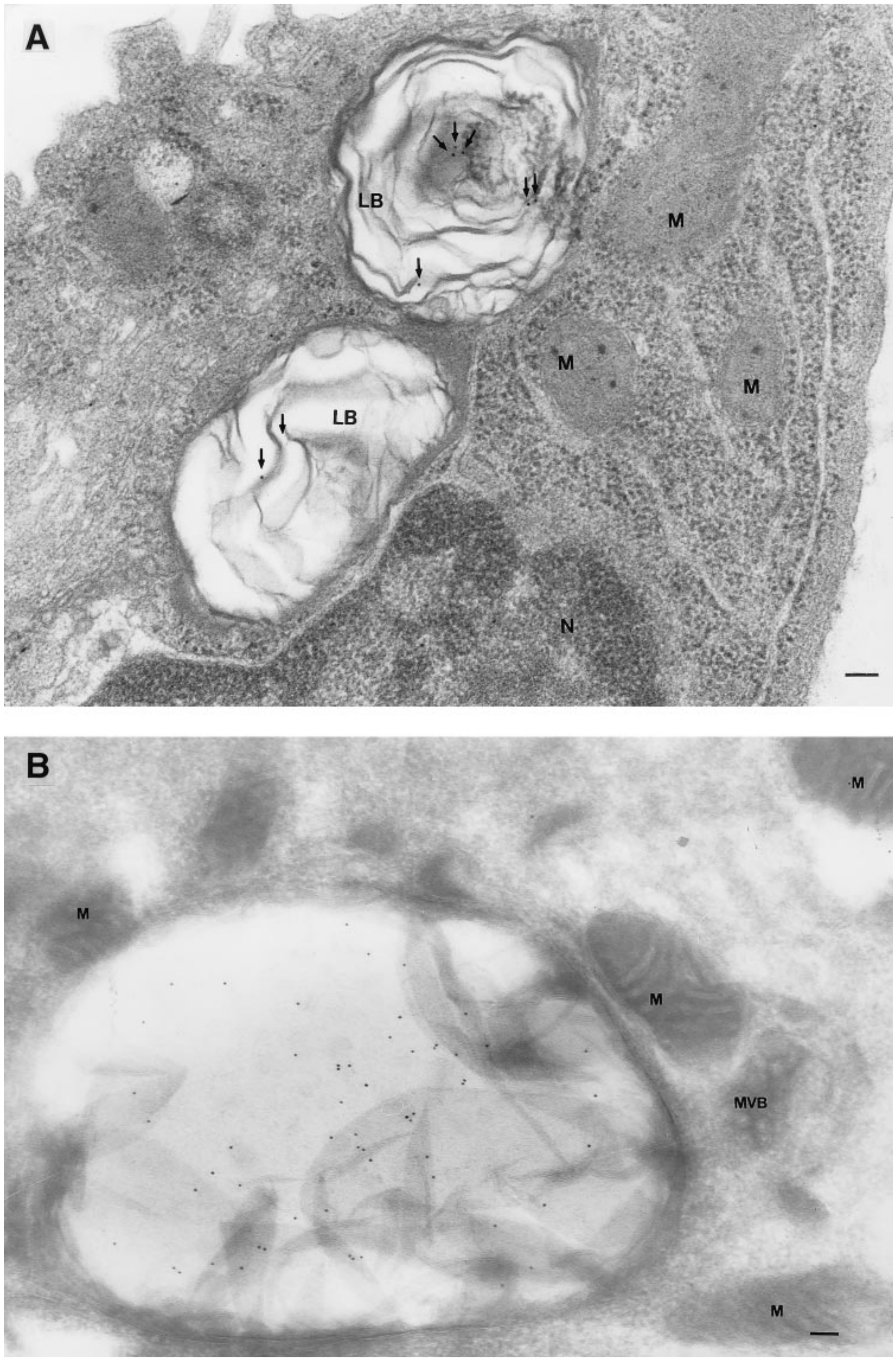

Fig. 5. Intracellular localization of endocytosed SP-A in type II pneumocytes. *A*: electron micrograph (Epon section) of type II pneumocyte after endocytosis of SP-A. After tracheal instillation of FITC-labeled SP-A for 5 min, Epon sections of the lung were incubated with the mouse anti-FITC antibody and goat anti-mouse antiserum conjugated with 12-nm large gold particles. Endocytosed SP-A is indicated by the immunogold particles (arrows). LB, lamellar body; N, nucleus; M, mitochondria. Bar, 0.1 μm. *B*: electron micrograph (thin cryosection) of SP-A-containing vesicles showing a closeup of large vacuolar vesicles containing remnants of smaller vesicles and lamellae after treatment with a mouse anti-FITC antibody and goat anti-mouse antiserum conjugated with 12-nm large gold particles as described above. Immunogold particles, indicating endocytosed SP-A, can be seen within the lumen. Cytosol, nucleus, mitochondria, and multivesicular bodies (MVB) are devoid of label. Mean size of the large vacuoles is 1.4 μm. Bar, 0.1 μm.

leagues (7, 8). Also, using CLSM, we could confirm in normal cells that although at 0 min all label is extracellular, after 3- 5 min, considerable amounts of SP-A and lipid could be found intracellularly in clathrin-positive vesicles. In contrast, in potassium-depleted cells, very little of these intracellular surfactant components could be seen. Also, the fine cell membrane lining pattern of the clathrin antibody in potassium-depleted cells seen in Fig. 3*C* was clearly different from that in normal cells. Furthermore, under potassium-depleted conditions, clathrin did not colocalize with either lipid or SP-A.

At early time points (≤10 min after the start of endocytosis), SP-A and lipid colocalized with the SP-A-binding protein BP55 in the same intracellular vesicles (Fig. 3). In combination, these data are compatible with the model described above in which lipid and SP-A internalize as one package via coated pits after binding to the SP-A receptor.

We could exclude some alternative explanations for the decrease in uptake of the surfactant components in potassium-depleted cells. *1*) The effect of potassium depletion on SP-A internalization could not be explained by differences in SP-A binding or receptor affinity (see RESULTS). *2*) Potassium depletion in some cell systems also affects other transport processes such as fluid-phase endocytosis. In our system however, uptake of the fluid-phase marker Lucifer yellow was not changed in potassium-depleted cells versus normal cells. Also, nonspecific lipid uptake was unaltered by potassium depletion (results not shown). *3*) Potassium depletion inhibits protein synthesis as first shown by Ledbetter and Lubin (18). To exclude that this would affect SP-A-mediated uptake, we performed lipid uptake experiments in the presence of 100 μM cycloheximide, a known protein synthesis inhibitor. We found no effect on lipid uptake for the first 2 h after addition of the inhibitor. Therefore, we feel that inhibition of protein synthesis is not responsible for the effect found. *4*) The ATP content of potassium-depleted cells was not different from that in control cells, suggesting that depletion of energy stores does not account for the effect found.

The small amounts of SP-A and lipid still internalized under potassium-depleted conditions despite inhibition of coated-pit function could be due to several reasons. After potassium depletion, some coated-pit structures were still detectable by electron microscopy. Other investigators (20) previously found that potassium depletion will inhibit formation of new coated pits, but coated pits already formed by the time the inhibition is started would still be able to internalize, thus allowing a small amount of ligand to internalize. Alternatively, a small amount of SP-A and lipid could also be taken up by pathways other than coated-pit internalization. As illustrated by Lucifer yellow uptake, under potassium-depleted conditions, endocytic pathways other than clathrin-mediated uptake are clearly functioning. Previously, Wissel et al. (29) showed that in our cell system a small fraction of lipid is taken up by one or more pathways that are not specific and not energy dependent. Uptake via these pathways takes place simultaneously with SP-A-mediated uptake and is not influenced by potassium depletion (see RESULTS). The extent of lipid internalization remaining under potassium depletion can be accounted for by these pathways. Caveola-mediated uptake seems unlikely because we could not detect caveolin-1 in freshly isolated type II cells (results not shown). The exact identity of these alternative pathways therefore remains unclear.

Our data are in contrast to those of Horowitz and colleagues (7, 8), who suggested that SP-A did not have an effect on lipid uptake or even had an adverse effect. The reasons for this difference are not clear, but there are several methodological differences between our system and that of Horowitz and colleagues, such as the cell type used (freshly isolated versus adherent cells or cell lines), the liposomes used (small unilamellar vesicles versus multilamellar vesicles; lipid composition), and the procedure used to prepare SP-A. In previous experiments on lipid uptake, corroborated by preliminary experiments on SP-A uptake (results not shown), Wissel et al. (29) found that in their hands, type II cells kept on plastic in culture for 18 h lost their ability to endocytose both components and also degraded substantially more internalized lipid. Also, in previous work, we found that simply washing the cells with medium did not remove ~80% of the total cell-associated label, which could be removed by more efficient procedures such as back exchange or washing with EDTA and fatty acid-free BSA. We therefore feel it is possible that material adhering to the cell membrane would falsify a correct estimation of internalization.

The identity of the vesicles involved in surfactant endocytosis is not absolutely clear. In Epon sections, most lamellar bodies but no other organelles contained significant gold particles (i.e., FITC-SP-A) at time points < 10 min after administration. With the same experimental conditions in frozen sections, FITC-SP-A up to 10 min after its administration was mainly localized within large vacuoles containing many vesicles of intermediate size. The results, therefore, would suggest that the vacuoles containing the densely packed vesicles correspond to the lamellar bodies visible in Epon sections in accordance with previously published work (26), demonstrating that the fine structure of lamellar bodies differs between Epon and thin frozen sections. In Epon sections, the dense network of membranes of lamellar bodies is arranged in a parallel orientation. In cryosections, they appear as densely packed vesicles.

It is intriguing, however, that the vesicles, which contained endocytosed SP-A at early time points, were not only EEA1 positive but also LAMP-1 negative as shown by CLSM and immunoelectron microscopy and were supported by the subcellular fractionation results (Table 2). This, therefore, would suggest that they are early endosomes and not lamellar bodies, which are reported to have late endosomal/lysosomal markers. Wasano and Hirakawa (27) found LAMP-1 on the limiting membrane of lamellar bodies. However, the weak labeling intensity demonstrated in that report may still be compatible with an early endosomal nature of the stained vacuoles. Furthermore, the vacuoles presented in that earlier study did not show the typical morphology of lamellar bodies due to the use of cryosections and were not labeled by endocytosed SP-A as performed in our experiments. Voorhout et al. (26) demonstrated on thin cryosections that biosynthetic SP-A and the lysosomal membrane protein CD63 colocalize within multivesicular bodies as well as within empty vacuoles, which they suggested to be lamellar bodies (26). In our experiments, endocytosed SP-A at early time points was targeted to LAMP-1-negative large vesicles. The results of our subcellular fractionation experiments would suggest that these early-labeling vesicles are contained within the 0.22–0.32 and 0.33–0.48 M fractions, therefore overlapping with the lamellar body-containing fractions found at 0.33–0.58 M. Alternatively, it is also possible that these vesicles might represent a different subpopulation of lamellar bodies containing endocytosed material existing next to another population of LAMP-1-positive lamellar bodies containing de novo synthesized SP-A as components of the secretory pathway. Previous work by others (26, 28) has indeed suggested that lamellar bodies might possess properties of both the biosynthetic and endocytic pathways. Whether and when these two populations meet and possibly fuse with each other is not known yet. More conclusive evidence must be obtained to prove this hypothesis.

Our in vitro results were confirmed by in vivo instillation studies in intact lungs. Significant qualitative differences between both systems were not detected. SP-A uptake in the in vivo rat lung system, however, was quantitatively somewhat more pronounced as judged from the amount of label found in the type II cells (results not shown). The time course and labeling patterns in our study are in agreement with previously published electron-microscopic work by Young and colleagues (33, 34).

The recent characterization of mice in which the SP-A gene was inactivated (13) seems in contrast to the in vitro findings described here, which would suggest some role for SP-A in the regulation of surfactant homeostasis. The SP-A knockout mice show no obvious disturbance of surfactant pool sizes. However, this does not argue against a role for SP-A in type II cell surfactant metabolism. Although the knockout model will tell what the organism can do without the protein that is ablated, it does not necessarily say much about the function of the protein itself. Also, as in other knockout models, the genetic background of the mice chosen may be important, e.g., different epidermal growth factor receptor knockout mice show very different phenotypes depending on the genetic background (21, 23). Third, it is well possible that redundant mechanisms compensating for the lack of SP-A exist. Last, the knockout model up to now has been used to describe overall surfactant homeostasis to which several cell types in addition to type II cells (e.g., macrophages) contribute. Those experiments, therefore, do not rule out a local role for SP-A on type II cells. Clearly, much more work needs to be done in vivo as well as in vitro to properly characterize the physiological regulation of surfactant metabolism.

In summary, the present study demonstrates the following points: *1*) SP-A and lipids are internalized via the coated-pit or coated-vesicle pathway, and *2*) at early time points, they are colocalized in the same intracellular vesicles the bear early endosomal markers. The processes of surfactant reuptake and recycling could be of biological and therapeutic significance. They might allow the lung to rapidly replenish its limited pools without having to resort to de novo synthesis, which is time consuming and energy expensive. More insight into the mechanisms involved will lead to more optimal surfactant substitution therapies in premature infants and adults with respiratory distress as well as to possibly more effective ways of introducing drugs and genes into the lung.

We thank Dr. Ekkehard Richter and Petra Klein (Institute of Biology, Humboldt University Berlin, Berlin, Germany) for help with the confocal laser scanning microscopy. We thank Dr. John Hutton (University of Colorado Health Sciences Center, Denver, CO) who provided us with the monoclonal antibody against LAMP-1.

This work was supported by Deutsche Forschungsgemeinschaft Grants Ste 459/4-1 and 4-2.

REFERENCES

1. **Benne CA, Kraaijeveld CA, van Strijp JAG, Brouwer E, Harmsen M, Verhoef J, van Golde LMG, and van Iwaarden JF.** Interactions of surfactant protein A with influenza A viruses: binding and neutralization. *J Infect Dis* 171: 335–341, 1995.
2. **Bretscher MS and Lutter R.** A new method for detecting endocytosed proteins. *EMBO J* 7: 4087–4092, 1988.
3. **Dobbs LG, Gonzalez R, and Williams MC.** An improved method for isolating type II cells in high yield and purity. *Am Rev Respir Dis* 134: 141–145, 1986.
4. **Duck-Chong CG.** The isolation of lamellar bodies and their membranous content from rat lung, lamb tracheal fluid and human amniotic fluid. *Life Sci* 22: 2025–2030, 1978.
5. **Goldstein JL and Brown MS.** Binding and degradation of low density lipoproteins by cultured human fibroblasts. Comparison of cells from a normal subject and from a patient with homozygous familial hypercholesterolemia. *J Biol Chem* 249: 5153–5162, 1974.
6. **Hawgood S, Benson BJ, and Hamilton RL Jr.** Effects of a surfactant-associated protein and calcium ions on the structure and surface activity of lung surfactant lipids. *Biochemistry* 24: 184–190, 1985.
7. **Horowitz AD, Kurak K, Moussavian B, Whitsett JA, Wert SE, Hull WM, McNanie J, and Ikegami M.** Preferential uptake of small-aggregate fraction of pulmonary surfactant in vitro. *Am J Physiol Lung Cell Mol Physiol* 273: L468–L477, 1997.
8. **Horowitz AD, Moussavian B, and Whitsett JA.** Roles of SP-A, SP-B, and SP-C in modulation of lipid uptake by pulmonary epithelial cells in vitro. *Am J Physiol Lung Cell Mol Physiol* 270: L69–L79, 1996.
9. **Jaworek D, Gruber W, and Bergmeyer H-U.** Adenosin-5′-diphosphat und Adenosin-5′-monophosphat. In: *Methoden der enzymatischen Analyse*, edited by Bergmeyer H-U. Berlin: Akademie Verlag, 1970, p. 2051–2055.
10. **Kalina M, McCormack FX, Crowley H, Voelker DR, and Mason RJ.** Internalization of surfactant protein A (SP-A) into lamellar bodies of rat alveolar type II cells in vitro. *J Histochem Cytochem* 41: 57–70, 1993.

11. **Kalina M and Socher R.** Internalization of pulmonary surfactant into lamellar bodies of cultured rat pulmonary type II cells. *J Histochem Cytochem* 38: 483–492, 1990.
12. **Kalina M and Socher R.** Endocytosis in cultured rat alveolar type II cells: effect of lysomorphotropic weak bases on the process. *J Histochem Cytochem* 39: 1337–1348, 1991.
13. **Korfhagen TR, Bruno MR, Ross GF, Huelsman K, Ikegami M, Jobe AH, Wert SE, Stripp BR, Morris RE, Glasser SW, Bachurski CJ, Iwamoto HS, and Whitsett JA.** Altered surfactant function and structure in SP-A gene targeted mice. *Proc Natl Acad Sci USA* 93: 9594–9599, 1996.
14. **Kuroki Y, Mason RJ, and Voelker DR.** Alveolar type II cells express a high-affinity receptor for pulmonary surfactant protein A. *Proc Natl Acad Sci USA* 85: 5566–5570, 1988.
15. **Kuroki Y, Mason RJ, and Voelker R.** Pulmonary surfactant apoprotein A structure and modulation of surfactant secretion by rat alveolar type II cells. *J Biol Chem* 263: 3388–3394, 1988.
16. **Larkin JM, Brown MS, Goldstein JL, and Anderson RGW.** Depletion of intracellular potassium arrests coated pit formation and receptor-mediated endocytosis in fibroblasts. *Cell* 33: 273–285, 1983.
17. **Larkin JM, Donzell WC, and Anderson RGW.** Potassium-dependent assembly of coated pits: new coated pits form as planar clathrin lattices. *J Cell Biol* 103: 2619–2627, 1986.
18. **Ledbetter MLS and Lubin M.** Control of protein synthesis in human fibroblasts by intracellular potassium. *Exp Cell Res* 105: 223–236, 1977.
19. **Ryan RM, Morris RE, Rice WR, Ciraolo G, and Whitsett JA.** Binding and uptake of pulmonary surfactant protein (SP-A) by pulmonary type II epithelial cells. *J Histochem Cytochem* 37: 429–440, 1989.
20. **Schmid SL and Carter LL.** ATP is required for receptor-mediated endocytosis in intact cells. *J Cell Biol* 111: 2307–2318, 1990.
21. **Sibilia M and Wagner EF.** Strain-dependent epithelial defects in mice lacking the EGF receptor. *Science* 269: 234–238, 1995.
22. **Stevens PA, Wissel H, Sieger D, Meienreis-Sudau V, and Rüstow B.** Identification of a new surfactant protein A binding protein at the cell membrane of rat type II pneumocytes. *Biochem J* 308: 77–81, 1995.
23. **Threadgill DW, Dlugosz AA, Hansen LA, Tennenbaum T, Lichti U, Yee D, LaMantia C, Mourton T, Herrup K, Harris RC, Barnard JA, Yuspa SH, Coffey RJ, and Magnuson T.** Targeted disruption of mouse EGF receptor: effect of genetic background on mutant phenotype. *Science* 269: 230–234, 1995.
24. **Tsuzuki A, Kuroki Y, and Akino T.** Pulmonary surfactant protein A-mediated uptake of phosphatidylcholine by alveolar type II cells. *Am J Physiol Lung Cell Mol Physiol* 265: L193–L199, 1993.
25. **Volz B, Orberger G, Porwoll S, Hauri H-P, and Tauber R.** Selective reentry of recycling cell surface glycoproteins to the biosynthetic pathway in human hepatocarcinoma HepG2 cells. *J Cell Biol* 130: 537–551, 1995.
26. **Voorhout WF, Veenendaal T, Haagsman HP, Weaver TE, Whitsett JA, van Golde LMG, and Geuze HJ.** Intracellular processing of pulmonary surfactant protein B in an endosomal/lysosomal compartment. *Am J Physiol Lung Cell Mol Physiol* 263: L479–L486, 1992.
27. **Wasano K and Hirakawa Y.** Lamellar bodies of rat alveolar type 2 cells have late endosomal marker proteins on their limiting membranes. *Histochemistry* 102: 329–335, 1994.
28. **Williams MC.** Uptake of lectins by pulmonary alveolar type II cells: subsequent deposition into lamellar bodies. *Proc Natl Acad Sci USA* 81: 6383–6387, 1984.
29. **Wissel H, Looman AC, Fritzsche I, Rüstow B, and Stevens PA.** SP-A-binding protein BP55 is involved in surfactant endocytosis by type II pneumocytes. *Am J Physiol Lung Cell Mol Physiol* 271: L432–L440, 1996.
30. **Wissel H, Zastrow S, Richter E, and Stevens PA.** Internalized SP-A and lipid are differentially resecreted by type II pneumocytes. *Am J Physiol Lung Cell Mol Physiol* 278: L580–L590, 2000.
31. **Wright JR, Borchelt JD, and Hawgood S.** Interaction of surfactant protein Mr 26kDa-36kDa (SP-A) with isolated alveolar type II cells (Abstract). *FASEB J* 2: 959, 1988.
32. **Wright JR, Borchelt JD, and Hawgood S.** Lung surfactant apoprotein SP-A (26–36 kDa) binds with high affinity to isolated alveolar type II cells. *Proc Natl Acad Sci USA* 86: 5410–5414, 1989.
33. **Young SL, Fram EK, Larson E, and Wright JR.** Recycling of surfactant lipid and apoprotein-A studied by electron microscopic autoradiography. *Am J Physiol Lung Cell Mol Physiol* 265: L19–L26, 1993.
34. **Young SL, Wright JR, and Clements JA.** Cellular uptake and processing of surfactant lipids and apoprotein SP-A by rat lung. *J Appl Physiol* 66: 1336–1342, 1989.
35. **Zimmer KP, Matsuda I, Matsuura T, Mori M, Colombo JP, Fahimi HD, Koch HG, Ullrich K, and Harms E.** Ultrastructural, immunocytochemical and stereological investigation of hepatocytes in a patient with the mutation of the ornithine transcarbamylase gene. *Eur J Cell Biol* 67: 73–83, 1995.